25th ABCM International Congress of Mechanical Engineering
October 20-25, 2019, Uberlândia, MG, Brazil

COB-2019-1636
CFD SIMULATION FOR THE VIV FORCE IN A CIRCULAR CYLINDER OSCILLATING PERPENDICULAR TO THE CURRENT

Paulo Oliveira Kiryu
University of Campinas, Graduate School of Petroleum Science and Engineering, Campinas-SP, Brazil
p137245@dac.unicamp.br

Caio Cesar de Oliveira Trigo
University of Campinas, LabRiser/ Center of Petroleum Studies, Campinas-SP, Brazil
ctrigo87@unicamp.br

Ricardo Franciss
Catholic University of Petropolis, Petropolis-RJ, Brazil
ricardo.franciss@ucp.br

Celso Kazuyuki Morooka
University of Campinas, Faculty of Mechanical Engineering & Center of Petroleum Studies, Campinas-SP, Brazil
morooka@unicamp.br

Abstract. *An oscillating circular cylinder perpendicular to the current is accounted, and two-dimensional numerical simulations through the Computational Fluid Dynamics (CFD) are taken. Hydrodynamics drag and lift forces on the cylinder are investigated. Commercial software was used and results are verified in terms of the drag and lift force coefficients with those in the literature to verify the computational model developed for simulations. Numerical simulations results are verified with experiments and discussions are focused on the overset grid approach which has been applied on CFD simulations. Good agreement was verified for hydrodynamic force coefficients calculated for the transversally oscillating cylinder to the incident current.*

Keywords: *Marine Riser, Subsea Pipeline, Vortex-induced Vibration, CFD, Current*

1. INTRODUCTION

In the offshore petroleum field production, oil and gas are pumped from the subsea wells at the seabed to the sea surface facility to be processed through rigid or flexible pipelines denominated as flowlines and risers. The petroleum receives the necessary treatment on board of floating production units (FPUs), and the oil and the gas are exported each one separately to the land through large relief oil tankers and/or subsea pipelines.

Risers, flowlines and pipelines are largely applied on the oil industry. Although the broad application of pipeline and risers by the oil industry, several issues are still remaining to be investigated due to environmental loads, as those from the sea current. As is well known, the flow around slender pipeline structures is a complex phenomenon, in particular those related to the vortex shedding and wake in the downstream. Due to the elastic response of the structure and the oscillatory nature of hydrodynamic fluid forces, this flow field causes the Vortex Induced Vibration (VIV) of the structure.

A lot of effort has been done in the past to investigate the vortex shedding around structures, as for instance, the investigation of the fluid flow around bluff bodies by Williamson and Roshko (1988).

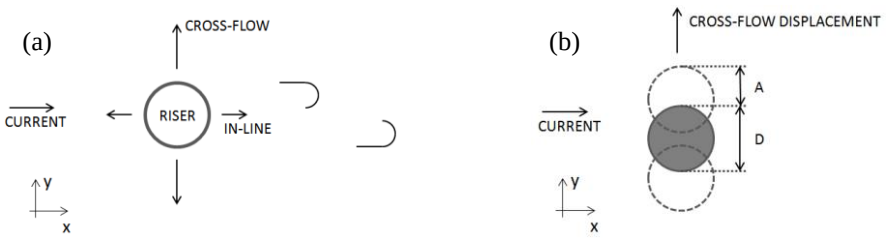

Figure 1. (a) In-line and cross-flow directions of vibration. (b) Motion in cross-flow direction.

The fluid flow around the circular cross section of a riser or pipeline is schematically shown in Fig. 1 (a). The total hydrodynamic fluid forces in the section can be decomposed in two perpendicular directions: one in the in-line direction with the incident current (drag, F_D); and another one in the cross-flow direction (lift, F_L). Figure 1 (b) shows the arrangement of a single cylinder section with cross-flow motion.

Vibrations can cause collisions between structures, and there is possibility of service life reduction due to the fatigue (Tsukada et al., 2008). The most critical configuration is when the frequency of excitation due to vortex shedding is close to the natural frequency of the structure.

Williamson and Roshko (1988) through an experimental investigation about the VIV and lock-in on a circular cylinder with diameter D, observed different patterns of vortex emissions according to the non dimensional amplitude of response (A/D) and reduced velocity (U_r), in the range of $0 < U_r < 15$.

Experiment was conducted in a towing tank (Arakaki et al., 2016) with a steel pipe vertically mounted and towed along the tank. Forced motion was produced perpendicular to the carriage advancement. The towing carriage advanced with constant speed and the pipe with D=0,0762m was oscillated with sinusoidal motion. Results of forces for different combinations of vibration amplitude (0,007m < A < 0,091m), forced frequency (0,2Hz < f < 1,59Hz) and carriage velocity were obtained (0,3m/s < V < 1m/s).

In the present paper, an oscillating circular cylinder perpendicular to the current is considered, and two-dimensional numerical simulations through CFD are conducted. Hydrodynamic drag and lift forces on the cylinder are investigated. Sensibility of different mesh and time step size (Δt) in the computational model is investigated and comparisons are shown. The overset grid approach is used for CFD simulations and results are compared with CFD results from traditional mesh and experimental results from Arakaki et al., (2016). Commercial software was used for the CFD simulations, and the drag and the lift force coefficients, respectively, were also verified with literature results. The main objective was to analyze advantages of the overset grid approach as a tool for building the mesh.

2. NUMERICAL SIMULATION

The software used was the ANSYS, the geometry of the fluid domain and the mesh was done in ANSYS Workbench, the simulations were carried out by ANSYS Fluent CFD. A two-dimensional oscillating cylinder section subjected to an incident current with uniform velocity profile (U_∞) was taken. The Reynolds number (Re) is indicated in Eq. (1):

$$Re = \frac{\rho U_\infty D}{\mu} \tag{1}$$

where, μ is the dynamic viscosity and ρ is the density of domain fluid. The Strouhal number (St) is given by Eq. (2), where f_s is the vortex shedding frequency, obtained from the time series of F_L.

$$St = \frac{f_s D}{U_\infty} \tag{2}$$

The drag coefficient and the lift coefficient are defined in Eq. (3) and Eq. (4), respectively.

$$C_D = \frac{F_D}{0{,}5\rho D {U_\infty}^2} \tag{3}$$

$$C_L = \frac{F_L}{0{,}5\rho D {U_\infty}^2} \tag{4}$$

where, the total fluid force F is calculated by the CFD simulation as the sum of pressure and viscous forces around the cylinder section, and decomposed in two perpendicular F_D and F_L forces. The forced motion is imposed to the cylinder perpendicularly to the incident current direction with amplitude (A) and a frequency (f). Experiment was carried out in a towing water tank (Arakaki et al, 2016) with a vertical pipe moving forward with constant speed and transversally imposed motions. The time series of sinusoidal motions in the experiment was recorded and it has been used for the numerical simulation.

2.1 Characteristics of the Fluid Domain

The Navier-Stokes equations for an incompressible viscous fluid flow and the conservation of mass and momentum are considered. The ANSYS Fluent CFD (ANSYS, 2018), based on the Finite Volume Method, is used. The fluid domain is divided into small volume elements and the Navier-Stokes equations are integrated in the each of those volumes.

Initially, consistency of the simulation result was verified for a stationary cylinder section case. The two-dimensional circular cylinder section was placed inside a rectangular computational domain with dimensions of 30D in

the in-line direction and 20D in the cross-flow one. The cylinder is centered in the cross-flow direction, 10D from the top and 10D from the bottom, as in Fig. 2.

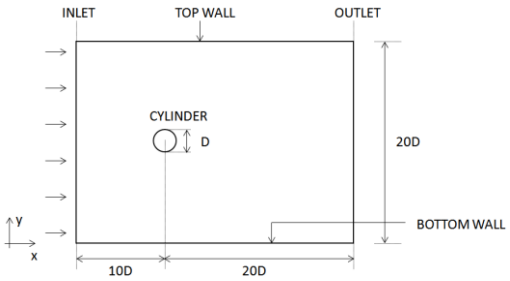

Figure 2. Two-dimensional fluid domain geometry.

The absolute fluid viscosity (μ) is 0,00108 Pa.s² and the density (ρ) is 1000 kg/m³. The fluid flow at inlet boundary has a uniform vertical profile with the horizontal velocity (U). Symmetry boundary conditions are used and the vertical (normal) velocity components at the upper and downward boundaries are respectively taken equal to zero.

2.2 Mesh generation

The mesh must be more refined nearby the cylinder outer surface, where the boundary layer and the vortex detachment occur. Another region in which mesh must be also refined is around the vortex shedding street at downstream from the cylinder to the fluid domain outlet (Saito and Morooka, 2010; Arakaki et al., 2015; Kiryu and Morooka, 2018).

In two-dimensional cases, a structured mesh presents planar cells with four edges, and an unstructured mesh can show various shapes of cells although they usually are triangular ones. For the boundary layer region, structured meshes are usually taken to get better resolution in the numerical simulations in comparison with the use of unstructured meshes with same number of cells. In the present study, the general mesh of the fluid domain is predominantly unstructured, and the mesh is structured nearby the boundary layer at the cylinder outer surface (Saito and Morooka, 2010)

In the present study, the overset grid approach accuracy was investigated. The overset grid is composed by a background mesh and a compound mesh. The compound mesh can move on top of the fixed background mesh, thus avoiding the grid-regeneration or the mesh distortion problems. The communication between the compound mesh and background mesh during body motion in the overset grid approach case occurs through interpolations of fluid values of cells at the overset interface. In the other hand, in the traditional approach of remeshing, many cells are created or deleted nearby the body surface where the number cells is increased, in order to have refinement of the mesh. For the present numerical simulations, the mesh dependency study was performed with a stationary cylinder and with traditional grid (without overset grid approach). Then, the cylinder was forced to oscillate in cross-flow direction and numerical simulations were done with overset grid approach. Figure 3 shows an overview of the two mesh types.

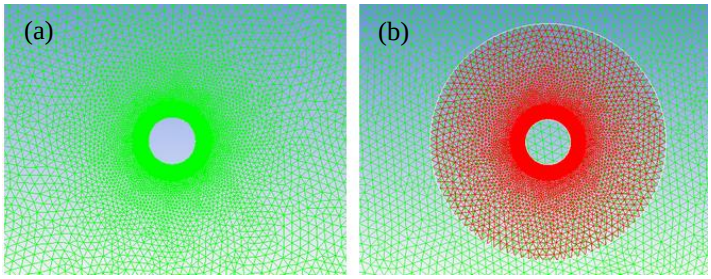

Figure 3. (a) Traditional grid approach. (b) Overset grid approach.

3. RESULTS

3.1 Stationary cylinder

Initially, the mean drag coefficient (C_{Davg}) and the root mean square (rms) of lift coefficient (C_{Lrms}), St and other details of the flow were calculated for the stationary cylinder and Δt was set to 0,005s.

The mesh dependency study was performed for the Re=63500 (U=0,9m/s), as in the Tab. 1. Mesh n. 4 has more cells than Mesh n. 3 and almost the same results of Mesh n. 3, so, it was decided to adopt the Mesh n. 3 for the simulations to avoid excessive computational efforts.

Table 1. Mesh dependency study results for Re=63500.

Mesh	Nodes	Elements	C_D	C_{Lrms}	St
1	14595	20889	1,03	0,83	0,25
2	50677	58795	0,89	0,58	0,24
3	55571	68541	0,90	0,62	0,24
4	79662	116636	0,91	0,62	0,24

Then, a study of the sensibility for the time step size was also carried out with the selected mesh size, concerning to C_{Davg}, C_{Drms}, C_{Lrms} and St. This analysis was done with two types of approach when building the mesh, the traditional and the overset meshes, and temporal discretization of the first order and second order. Results are shown in Figures 4 and 5 in which Δt_{min}=0,0002s is the finest time step in these calculation and Δt is the time step used in the analyzed calculation. Square marks are the traditional grid approach results with temporal discretization of second order, triangles marks are the traditional grid approach with temporal discretization of first order, and finally, circle marks are the overset grid approach with temporal discretization of first order. The temporal discretization of second order for the overset mesh approach was not done as it is not recommended by the user guide (ANSYS, 2018). The main objective of this analysis was to compare results from the overset grid and the traditional grid approaches. The overset grid approach is applied later on cases of the oscillating cylinder.

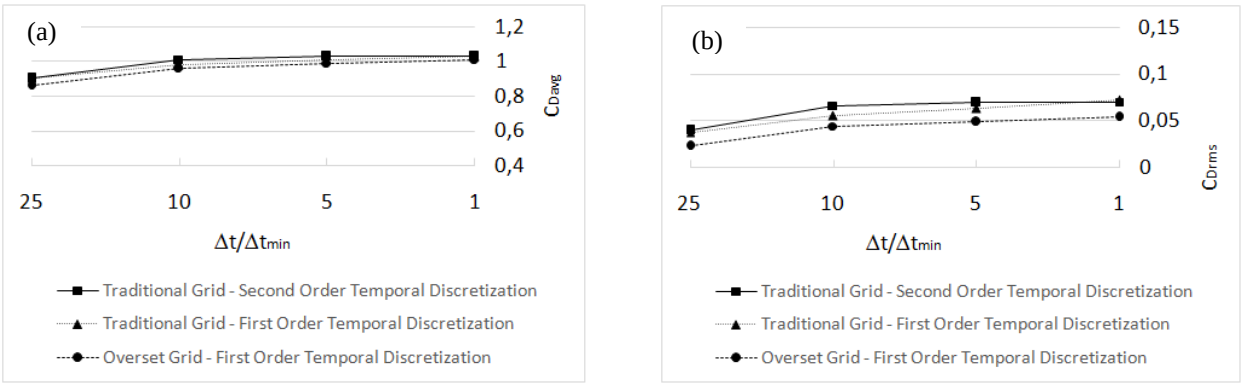

Figure 4. Time step size analysis of traditional grid with first and second order discretizations, and overset grid with first order discretization. Re=63500. (a) C_{Davg}. (b) C_{Drms}.

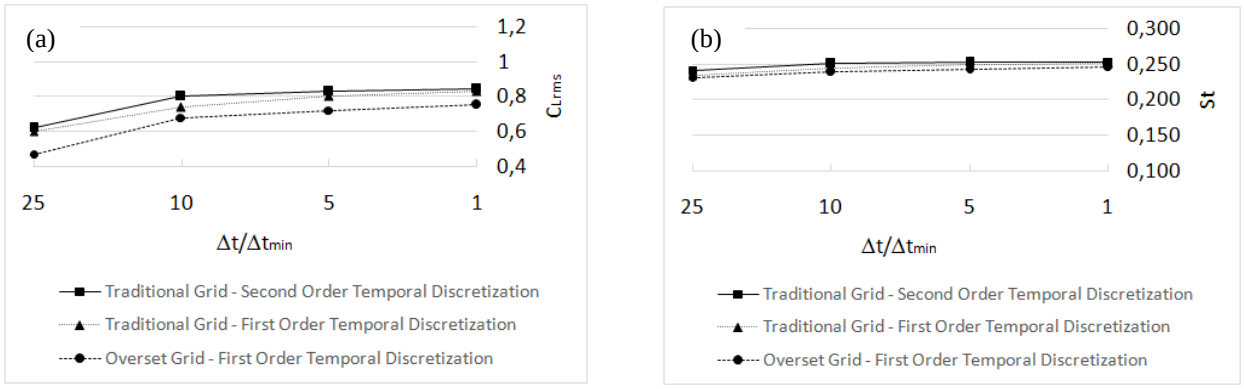

Figure 5. Time step size analysis of traditional grid with first and second order discretizations, and overset grid with first order discretization. Re=63500. (a) C_{Lrms}. (b) St.

The time step of Δt=0,001s ($\Delta t/\Delta t_{min}$=5) was adopted for further simulations. Although the time step of Δt=0,0002s ($\Delta t/\Delta t_{min}$=1) gives a bit better result it does not justify the larger computational time effort needed for simulations. It is also clear that cases with the overset grid approach also follow the tendency observed for simulation results with

traditional mesh, therefore, the advantages of the overset grid can be exploited in some cases like moving bodies simulations where the traditional grid results in problems due to low convergence or high computational effort.

Figure 6 shows the instantaneous vorticity contour fields for the two mesh types (Fig. 3) at the flow-time (t=10s). Contours in Fig. 6 (a) were obtained for the traditional mesh, and for the overset grid approach is shown in Fig. 6 (b).

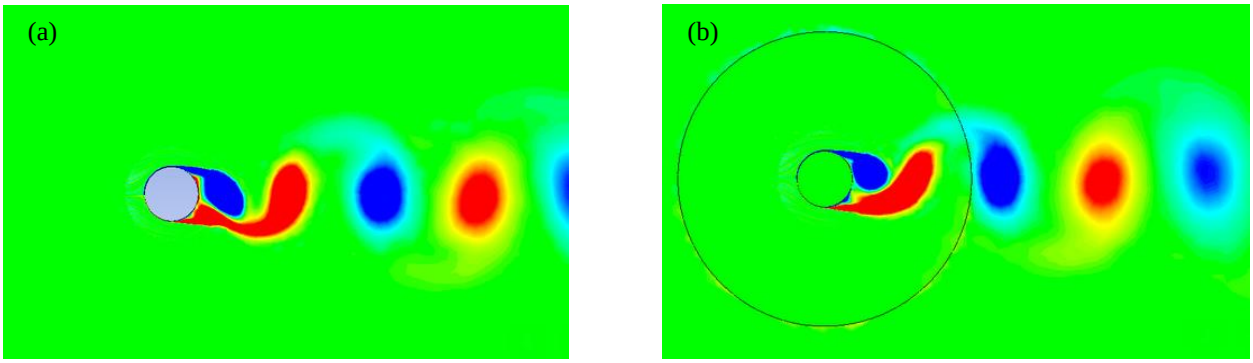

Figure 6. Vorticity contour field from (a) traditional grid, and (b) overset grid. Re=63500 and t=10s.

Occurrence of small vorticities can be verified in Fig. 6 (b), around the overset boundary (the external black circle) where communication between the component mesh and background mesh occurs, the overset boundary is obtained by showing the superposition of the component mesh above the background mesh in the post-processing. It suggests that some interference in calculations occurs due to interpolations done in simulations over the two grids, although no significant influence could be observed in the results.

3.2 Oscillating cylinder

Simulations were conducted with the cylinder forced to oscillate. First of all, a similar case by considering same parameters of the experiment, with A=0,0762m (A/D=1), U=0,9m/s and f=1,205Hz was carried out by the overset grid and the remeshing (dynamic mesh with traditional grid) approaches, respectively. For the remeshing approach, the time step size was reduced to 0,0005s due to difficulties in the numerical convergence with the time step of 0,001s and problems observed due to remeshing process with the movement of the cylinder. The flow features, force coefficients, shedding frequencies were obtained from the CFD simulations, and results are compared with experimental ones (Arakaki et al., 2016).

Figures 7 (a), 8 (a) and 9 (a) show the time history of C_D and Figs. 7 (b), 8 (b) and 9 (b) the time history of C_L. In Figure 7, CFD results are with the remeshing approach, the Figure 8 refers to CFD results with the overset grid approach, and finally, in Figure 9 results from experimental are shown.

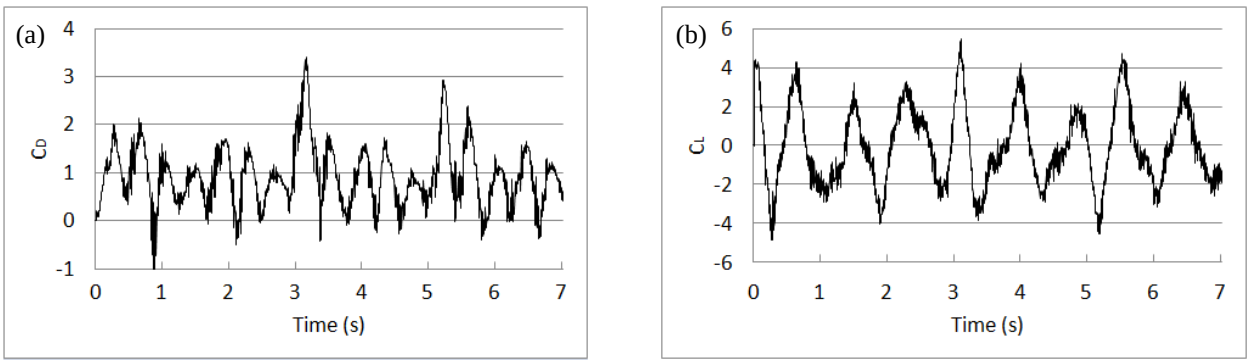

Figure 7. Time history of the force coefficients for oscillating cylinder with remeshing approach, A/D=1, T=0,83s and Re=63500. (a) C_D. (b) C_L.

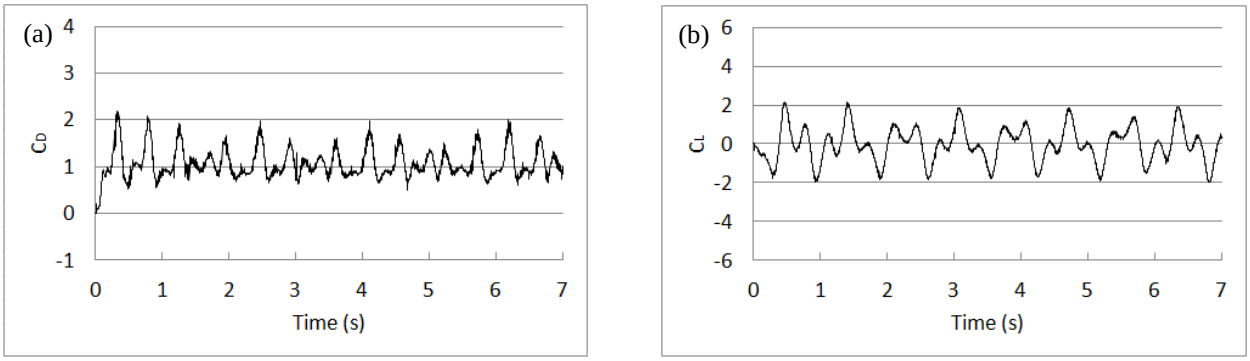

Figure 8. Time history of the force coefficients for oscillating cylinder with overset grid approach, A/D=1, T=0,83s and Re=63500. (a) C_D. (b) C_L.

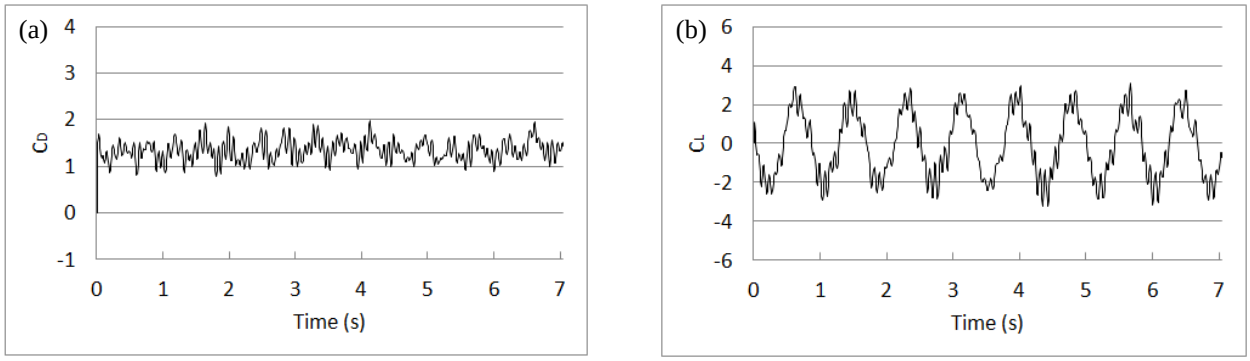

Figure 9. Time history of the force coefficients for oscillating cylinder from the experiment, A/D=1, T=0,83s and Re=63500. (a) C_D. (b) C_L.

Figure 10 shows the frequency spectrum. The first peak of C_L from the simulations and from the experiment is f=1,2Hz, the same frequency of forced motion, the others peaks in the CFD simulations are the vortex shedding frequencies.

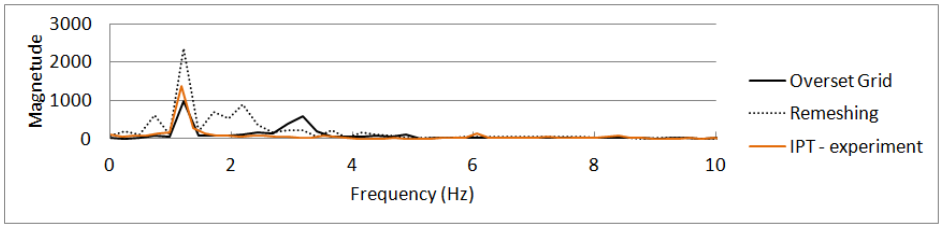

Figure 10. FFT of C_L at forced motion. A/D=1, T=0,83s and Re=63500.

Table 2 shows a summary of C_{Davg}, C_{Lavg}, C_{Drms}, C_{Lrms} from the previous Figures 7, 8 and 9. Frequencies (f_1 and f_2) for the C_L were obtained by fast Fourier transform (FFT). From results in the Tab. 2, the overset grid results show better agreement with the experimental ones (Arakaki et al., 2016). Moreover, it was observed that computer simulation time for the traditional grid took twice time of the overset grid.

Table 2. Comparison for C_L frequency at forced motion. A/D=1, T=0,83s and Re=63500.

	Remeshing	Overset	Experiment (Arakaki et al., 2016)
C_{Davg}	0,92	1,05	1,35
C_{Drms}	0,67	0,26	0,22
C_{Lavg}	0,04	0,04	-0,07
C_{Lrms}	1,95	0,88	1,64
f_1 (Hz)	1,2	1,2	1,2
f_2 (Hz)	2,3	3,0	-
Δt (s)	0,0005	0,001	0,01

Finally, four simulations were carried out just with overset grid approach, four oscillation periods (T) were studied (T=1,25s, T=1,00s, T=0,91s and T=0,67s), A/D=0,8 and Re=28222, the values were compared with literature as shown in Tab. 3, where f_1, f_2, f_3, f_4 and f_5 are the frequencies in ascending order obtained by the time series of C_L.

Table 3. Comparison for C_L frequency at forced motion. A/D=0,8 and Re=28222.

	T=1,25s		T=1,00s		T=0,91s		T=0,67s	
	CFD	Exp.	CFD	Exp.	CFD	Exp.	CFD	Exp.
C_{Davg}	1,32	2,28	1,73	1,79	2,24	1,73	2,42	1,61
C_{Drms}	0,32	0,57	0,54	0,99	0,73	1,11	1,31	2,05
C_{Lavg}	0,11	-0,027	-0,75	-0,12	-0,77	-0,27	-0,007	-0,53
C_{Lrms}	23	4,84	20	7,67	18	8,53	15,23	16,6
f_1 (Hz)	0,8	0,8	1	1	1,1	1,1	1,5	1,5
f_2 (Hz)	2,4	5,6	5	5	5,5	5,5	7,4	4,5
f_3 (Hz)	4	7,1	7	7	7,7	7,7	10,4	7,5
f_4 (Hz)	5,6	8,8	10,9	-	12,1	-	13,4	-
f_5 (Hz)	7,2	-	13	-	14,3	-	19,4	-
Δt (s)	0,001	0,01	0,001	0,01	0,001	0,01	0,001	0,01

From the cases of Tab. 3, the overset grid approach captured the frequency (f_1) of the lift force from vibration motion for all oscillation periods analyzed, since f_1 shows total agreement with experimental values (1/T). Other frequencies (f_2, f_3, f_4 and f_5) are due to the flow action (like vortex shedding) on the lift force and some of them are similar to the experimental frequencies as, for example, in T=1,00s and T=0,91s where $f_{3CFD}=f_{3Exp}$ and $f_{4CFD}=f_{4Exp}$, it shows the capability of the CFD model to capture vortex shedding frequencies from the flow. More investigation is needed regarding the lift force due to discrepancies against experimental values.

4. CONCLUSIONS

In present work, a computational model was developed for the fluid flow around a cylinder forced to oscillate perpendicularly to the incident current direction. Two-dimensional CFD numerical simulations were performed and simulation performance was verified for different mesh types.

The overset grid approach has shown better results with reduced computer simulation time when compared with the remeshing (traditional) approach which took twice computation time of the overset grid approach. The remeshing approach presented more difficulties for the numerical convergence to get the result, and problems due to remeshing process with the cylinder moving was also increased.

It could be also observed that overset grid approach besides reducing the computational time, contributed to simplify the mesh building process. Numerical simulation results were also compared with the experiment, and in general, overset grid results presented better agreement with experimental ones.

As future steps, more CFD simulations should be performed for different Re numbers taking advantages observed for the overset grid approach, for instance, by varying the amplitude and frequency of the cylinder motion.

5. ACKNOWLEDGEMENTS

The first author acknowledges Capes for the scholarship. Authors also thank CNPq, and UNICAMP/ FEM&Cepetro and PPG-CEP, for the continuing support for the research and academics.

6. REFERENCES

ANSYS, 2018. *User's Manual*. Version 18, SAS IP Inc.

Arakaki Junior, H.; Fontoura, D.V.R.; Nunhez, J.R.; Morooka, C.K., 2015. "Simulations of Current Forces on a Pipeline in Free Span through the Computational Fluid Dynamics", *23rd ABCM International Congress of Mechanical Engineering, COBEM 2015*, Rio de Janeiro, Brazil.

Arakaki Junior, H.; Trigo, C.C.O., Morooka, C.K.. "*Ensaios com Modelo Reduzida de Tubo*", Internal Report, UNICAMP, Campinas; 2016.

Kiryu, P.O.; Morooka, C.K., 2018. "Numerical Simulation of the Flow Over One and Two Circular Cylinders with Freedom to Move in Tandem", *27th International Congress on Waterborne Transportation, Shipbuilding and Offshore Constructions*, SOBENA 2018, Rio de Janeiro, Brazil.

Saito, J.S.; Morooka, C.K., 2010. "*Simulação Computacional do Escoamento em Torno de Uma Seção de um Duto Marítimo*", *VI National Congress of Mechanical Engineering, CONEM 2010*, Campina Grande, Brazil.

Tsukada, R.I.; Morooka, C.K.; Cechinel, R.O.; Matt, C.G.C., 2008. "*Estudo da Vibração em Duto Submarino Devido a Efeitos de Correnteza*", *22nd International Congress on Waterborne Transportation, Shipbuilding and Offshore Constructions, SOBENA 2008*, Rio de Janeiro, Brazil.

Williamson, C.H.K. and Roshko, A., 1988. "Vortex Formation in the Wake of an Oscillating Cylinder", *Journal of Fluids and Structures*, Vol. 2, pp. 355–381.

7. RESPONSIBILITY NOTICE

The authors are the only responsible for the printed material included in this paper.